DEUTSCHES ELEKTRONEN-SYNCHROTRON DESY

DESY 88-146
October 1988

Scaling Laws and Triviality Bounds in the Lattice ϕ^4 Theory III. n-component model

M. Lüscher
Deutsches Elektronen-Synchrotron DESY, Hamburg

P. Weisz
Max-Planck-Institut für Physik und Astrophysik, München

ISSN 0418-9833

NOTKESTRASSE 85 · 2 HAMBURG 52

To be sure that your preprints are promptly included in the
HIGH ENERGY PHYSICS INDEX ,
send them to the following address (if possible by air mail) :

DESY
Bibliothek
Notkestrasse 85
2 Hamburg 52
Germany

DESY 88-146
October 1988

ISSN 0418-9833

Scaling Laws and Triviality Bounds in the Lattice ϕ^4 Theory

III. n-component model

M. Lüscher
Deutsches Elektronen-Synchrotron DESY, Hamburg

P. Weisz
Max Planck Institut für Physik und Astrophysik, München

October 11, 1988

Abstract

Our previous analytic treatment of the 1-component standard lattice ϕ^4 theory in 4 dimensions is extended to the O(n) symmetric model. Particular attention is paid to the phenomenologically interesting case of $n = 4$. The renormalization group trajectories in the symmetric and in the Goldstone phase are mapped out and bounds on the renormalized self-coupling as a function of the ultra-violet cutoff are determined. Since the import of the results obtained has already been discussed in detail elsewhere, the emphasis here is put on the technical aspects of our work.

1. Introduction

In two previous articles [1,2], which will be referred to as (I) and (II) in the following, we have solved the standard lattice ϕ^4 theory in 4 dimensions in the sense that it was shown that most low energy physical quantities can be calculated with reasonable accuracy for all values of the bare parameters apart from a certain region in the broken symmetry phase, which is away from the critical line and which is therefore uninteresting from the point of view of the continuum limit (the ultra-violet cutoff is as low as the physical scales there). In this paper we extend the analysis to the O(n)-symmetric theory, the linear σ-model. A short account of this work has already been published in ref.[5] along with a discussion of the physical import of the results obtained. Furthermore, the basic ideas of our methods have been reviewed recently [3] so that here we assume the reader is familiar with our approach and concentrate on the presentation of the technical details of the computations (refs.[3,5] also contain a rather complete list of earlier references on the subject).

As compared to the one-component model, the solution of the O(n)-symmetric model is not much more difficult, in particular, the basic strategy followed in (I) and (II) carries over literally. In the symmetric phase, the main problem was that the high-temperature expansion coefficients for the renormalized mass m_R, the renormalized coupling g_R and the wave function renormalization constant Z_R had to be worked out to a high order. It is this step of the calculation which mainly accounts for the long time delay between completion of the $n = 1$ case and the general n case treated here. The derivation of the series, which we carried out to 14'th order, has been described in a separate publication [4]. In the broken symmetry phase, the presence of (massless) Goldstone bosons for $n \geq 2$ gives rise to a number of complications. In particular, not all renormalization conditions can be imposed at zero momentum. While this is not a fundamental difficulty, it is an inconvenience, especially in perturbation theory where one has to evaluate Feynman diagrams with non-zero external momenta if one wants to calculate the Callan-Symanzik β-function, for example.

This paper is divided into basically two parts, the first one (sect.3) dealing with the symmetric phase and the second (sect.4) with the Goldstone phase. Some common notation is summarized in sect.2 and a number of technical details, e.g. results on the Callan-Symanzik coefficients, are relegated to

appendices. In sect.4, we also include a discussion of finite cutoff effects, the aim being to determine the energy beyond which, in basic processes, the lattice cutoff significantly influences the amplitudes.

In the past two years or so, a major effort has been made to establish the triviality bound on the renormalized coupling in the Goldstone phase of the O(4) symmetric model by numerical simulation [11-18], using different approaches and, in one case, also different types of lattices to probe for the universality of the bound [16-18] (forerunners of these studies are [9, 10]). Thus, a detailed comparision with our analytical results is possible, the outcome being that there is almost perfect agreement within errors (see subsect.4.6; for a comparision with numerical work in the symmetric phase [11-13], see subsect.3.3). We would like to stress that the analytical and numerical analyses, which both have distinct systematic error sources, do not stand in competition but complement one another in the goal of attaining a correct and complete understanding of the model. Indeed they can even be combined in various ways to yield even more precise results, although this has as yet not been fully exploited.

Acknowledgements: Most of the material of this paper was completed before July 1988. During this time one of the authors (P.W.) was at SCRI, Tallahassee, and he would like to take this opportunity to thank the staff and colleagues at SCRI for their help and support. We are also indebted to C.B. Lang, G. Bhanot and J. Kuti for sending us detailed tables of the Monte Carlo data on the four-component model, which their collaborations [12,15,16] have recently produced.

2. Basic definitions

We consider the theory of real n-component scalar fields $\phi_\alpha(x)$ ($\alpha = 1,...,n$, $x \in \mathrm{Z}^4$) on a hypercubic lattice, which is specified by the action

$$S_h = S - h\sum_x \phi_n(x), \tag{2.1}$$

where the O(n)-symmetric part S is given by [1]

$$S = \sum_x \Big\{ -\kappa \sum_{\mu=0}^{3} \big(\phi(x)\cdot\phi(x+\hat{\mu}) + \phi(x)\cdot\phi(x-\hat{\mu})\big) + \phi(x)\cdot\phi(x) + \lambda(\phi(x)\cdot\phi(x)-1)^2 \Big\}. \tag{2.2}$$

Our final results will be quoted in the limit of vanishing "magnetic" field h, however at some intermediate stages we will also consider the theory with $h > 0$. The hopping parameter κ, which plays the rôle of the bare mass, and the coupling λ are restricted to non-negative values. In the context of the theory of electro-weak interactions, the interesting case is $n = 4$, but most of our calculations were done for general n and we thus keep $n \geq 2$ as a free parameter at this stage. The model is studied for all values of λ, including the limit $\lambda \to \infty$, where it reduces to the non-linear sigma model. Expectation values are defined in the conventional way.

The system above (for given n and $h = 0$) is known to possess two phases separated by a second order phase transition, the phase boundary being specified by a line $\kappa = \kappa_c(\lambda)$ in the space of bare parameters. For $\kappa < \kappa_c$ the system is in the symmetric phase, the S-matrix is O(n) invariant and the spectrum has a mass gap. For $\kappa > \kappa_c$, on the other hand, the O(n) symmetry is spontaneously broken and the field ϕ_n acquires a non-vanishing vacuum expectation value v. Moreover, the spectrum has $n-1$ Goldstone bosons and a resonance which we will refer to as the σ-meson.

As in the case $n = 1$, the composite field

$$\mathcal{O}(x) = \sum_{\mu=0}^{3} \big(\phi(x)\cdot\phi(x+\hat{\mu}) + \phi(x)\cdot\phi(x-\hat{\mu})\big), \tag{2.3}$$

plays an important rôle in the renormalization group analysis. We then consider the generating functional $W[H,K]$ defined by

$$\mathrm{e}^W = \frac{1}{Z_h}\int \prod_{x,\alpha} d\phi_\alpha(x) \exp\{-S_h + \sum_x [H(x)\cdot\phi(x) + K(x)\mathcal{O}(x)]\}, \tag{2.4}$$

where

$$Z_h = \int \prod_{x,\alpha} d\phi_\alpha(x) \exp\{-S_h\}. \tag{2.5}$$

[1] Here and below, the lattice spacing a is set equal to 1. $\hat{\mu}$ denotes the unit vector in the positive μ-direction.

With these conventions, $W[0,0] = 0$ and the vacuum expectation value v of ϕ_n is given by

$$v = \left.\frac{\partial W}{\partial H_n(x)}\right|_{H=K=0}. \tag{2.6}$$

In the symmetric phase, v vanishes proportional to h for $h \to 0$, while in the broken symmetry phase it approaches some positive value.

Next, we introduce a local magnetization $M_\alpha(x)$ through

$$M_\alpha(x) = \frac{\partial W}{\partial H_\alpha(x)} - v\delta_{\alpha n}, \tag{2.7}$$

and the Legendre transform $\Gamma[M,K]$ of $W[H,K]$ by

$$\Gamma = W - \sum_{x,\alpha} H_\alpha(x)(M_\alpha(x) + v\delta_{\alpha n}), \tag{2.8}$$

where as usual H is to be eliminated in favour of M by solving eq.(2.7). Then the bare vertex functions $\Gamma^{(k,l)}(p_1,...,p_k;q_1,...,q_l)_{\alpha_1...\alpha_k}$ of the fields ϕ_α and $\mathcal{O}$ are generated by expanding $\Gamma[M,K]$ in powers of the Fourier transforms $\tilde{M}_\alpha(p)$ and $\tilde{K}(q)$ of M_α and K as in eq.(I.2.9). In particular we have

$$\Gamma^{(0,0)} = \Gamma^{(1,0)}_\alpha = 0 \tag{2.9}$$

by definition.

3. Analysis in the symmetric phase

3.1 Renormalization Conditions

In the symmetric phase $\kappa < \kappa_c$, we consider only the limit $h = 0$. The O(n)-symmetry of the vertex functions then implies that $\Gamma^{(k,l)} = 0$ for k odd. It is convenient to impose renormalization conditions on the vertex functions at zero external momenta. The formulae are as for the case $n = 1$ except for the additional Clebsch-Gordan factors. A renormalized mass m_R and the wave function renormalization constant Z_R are defined through the behaviour of the negative inverse propagator at zero momentum, viz.

$$\Gamma^{(2,0)}(p,-p)_{\alpha\beta} = -\delta_{\alpha\beta}Z_R^{-1}\{m_R^2 + p^2 + O(p^4)\}, \qquad (p \to 0). \tag{3.1}$$

The renormalized coupling g_R is specified by

$$\Gamma^{(4,0)}(0,0,0,0)_{\alpha\beta\gamma\delta} = -\frac{1}{3}C_4(\alpha,\beta,\gamma,\delta)Z_R^{-2}g_R, \tag{3.2}$$

where

$$C_4(\alpha,\beta,\gamma,\delta) = \delta_{\alpha\beta}\delta_{\gamma\delta} + \delta_{\alpha\gamma}\delta_{\beta\delta} + \delta_{\alpha\delta}\delta_{\beta\gamma}. \tag{3.3}$$

Finally the renormalization constant $Z_R^{\mathcal{O}}$ associated with the composite field $\mathcal{O}$ is determined by

$$\Gamma^{(2,1)}(0,0;0)_{\alpha\beta} = \delta_{\alpha\beta}(Z_R Z_R^{\mathcal{O}})^{-1}, \tag{3.4}$$

and renormalized vertex functions $\Gamma_R^{(k,l)}$ are introduced in the usual way (eqs.(I.4.1)-(I.4.3)).

3.2 Scaling Laws

The derivation of the Callan-Symanzik equation proceeds exactly as in the case $n = 1$ (cf. sect.4.3 of (I)). In particular, the associated renormalization group functions β, γ, δ and ϵ are again given by eqs.(I.4.21)-(I.4.25). Their perturbative expansions up to three loops are tabulated, for general n, in appendix A.

The scaling laws which describe the behaviour of the coupling g_R and other quantities of interest in the limit $m_R \to 0$, λ fixed, are obtained by integrating eqs.(I.4.26)-(I.4.29). As will be verified later on, the relevant initial data for g_R are in the perturbative regime so that for all λ, g_R is forced to zero as $m_R \to 0$ according to the asymptotic formula

$$m_R = C_1(\beta_1 g_R)^{-\beta_2/\beta_1^2} e^{-1/\beta_1 g_R}\{1 + O(g_R)\}, \tag{3.5}$$

where β_1 and β_2 are the one- and two-loop coefficients of the β-function. The renormalization constant Z_R, on the other hand, tends to a constant,

$$Z_R = C_2\{1 + O(g_R)\}, \tag{3.6}$$

and for $Z_R^{\mathcal{O}}$ we have

$$Z_R^{\mathcal{O}} = C_3(g_R)^{\delta_1/\beta_1}\{1 + O(g_R)\} \tag{3.7}$$

(δ_1 denotes the one-loop coefficient of the δ-function). Finally, the approach of κ to the critical value κ_c is described by

$$\kappa_c - \kappa = C_3 m_R^2 (g_R)^{\delta_1/\beta_1}\{1 + O(g_R)\}. \tag{3.8}$$

In these equations, C_1, C_2 and C_3 are integration constants depending on λ.

If we use $\tau = 1 - \kappa/\kappa_c$ as the independent variable (instead of m_R), eqs.(3.5)-(3.8) yield the the well-known scaling laws [6]

$$m_R \underset{\tau\to 0}{\sim} C_4 \tau^{1/2} |\ln \tau|^{\delta_1/2\beta_1}, \tag{3.9}$$

$$g_R \underset{\tau\to 0}{\sim} \frac{2}{\beta_1} |\ln \tau|^{-1}, \tag{3.10}$$

$$Z_R \underset{\tau\to 0}{\sim} C_2, \tag{3.11}$$

$$Z_R^{\mathcal{O}} \underset{\tau\to 0}{\sim} C_5 |\ln \tau|^{-\delta_1/\beta_1}. \tag{3.12}$$

3.3 High-Temperature Series Analysis

For small correlation lengths $\xi = m_R^{-1}$, the quantities m_R, g_R, Z_R and $Z_R^{\mathcal{O}}$ can be calculated to high orders in the "high-temperature" (i.e. small κ) expansion. For our purposes it suffices to calculate the susceptibilities χ_2, μ_2 and χ_4, which are defined by

$$\delta_{\alpha\beta}\,\chi_2 = \sum_x \langle \phi_\alpha(x)\phi_\beta(0)\rangle, \tag{3.13}$$

$$\delta_{\alpha\beta}\,\mu_2 = \sum_x x^2 \langle \phi_\alpha(x)\phi_\beta(0)\rangle, \tag{3.14}$$

$$\frac{1}{3} C_4(\alpha,\beta,\gamma,\delta)\,\chi_4 = \sum_{x,y,z} \langle \phi_\alpha(x)\phi_\beta(y)\phi_\gamma(z)\phi_\delta(0)\rangle^{con}. \tag{3.15}$$

The quantities m_R, g_R, Z_R and $Z_R^{\mathcal{O}}$ are related to the above precisely as given in eqs.(I.6.7)-(I.6.10). For our previous work on the $n = 1$ case we were fortunate to be able to use the 10'th order series for these quantities derived and tabulated by Baker and Kincaid [22]. However, for the cases $n > 1$ no comparatively long series have (to our knowledge) been published. Using the linked-cluster expansion we have thus calculated the series to 14'th order for general n and λ, and for lattice dimensions 2,3 and 4 [4]. The results are available as computer files, which can be obtained per electronic mail from the authors.

As in the $n = 1$ case we prefer to present our results in terms of the bare coupling $\bar\lambda$ defined using the connected 1-site functions $\overset{\circ}{m}{}_i^{con}$ (see ref. [4],

Table 1: Values of λ and κ_c for given $\bar\lambda$ in the case $n = 4$

$\bar\lambda$	λ	κ_c
0.00	0.00	0.12500(2)
0.01	$1.7235 \cdot 10^{-3}$	0.12615(3)
0.02	$3.5656 \cdot 10^{-3}$	0.12733(3)
0.03	$5.5345 \cdot 10^{-3}$	0.12854(3)
0.04	$7.6391 \cdot 10^{-3}$	0.12979(3)
0.05	$9.8889 \cdot 10^{-3}$	0.13107(3)
0.06	$1.2294 \cdot 10^{-2}$	0.13239(3)
0.07	$1.4866 \cdot 10^{-2}$	0.13375(3)
0.08	$1.7616 \cdot 10^{-2}$	0.13514(3)
0.09	$2.0558 \cdot 10^{-2}$	0.13658(3)
0.10	$2.3705 \cdot 10^{-2}$	0.13806(3)
0.20	$7.0409 \cdot 10^{-2}$	0.15537(3)
0.30	$1.6348 \cdot 10^{-1}$	0.17765(4)
0.40	$3.4514 \cdot 10^{-1}$	0.20401(4)
0.50	$6.7905 \cdot 10^{-1}$	0.23123(5)
0.60	1.2559	0.25544(5)
0.70	2.2445	0.27441(5)
0.80	4.1270	0.28798(6)
0.90	9.3465	0.29727(6)
1.00	∞	0.30411(6)

eqs.(3.25)-(3.27)) by

$$\bar\lambda = -(1 + \frac{n}{2}) \overset{\circ}{m}{}_4^{con} / (\overset{\circ}{m}{}_2^{con})^2. \tag{3.16}$$

$\bar\lambda$ is a strictly monotonic function of λ rising from 0 to 1 in the range $0 \le \lambda \le \infty$. Furthermore, at small λ we have,

$$\bar\lambda = (n+2)\lambda \left\{1 - (3n+8)\lambda + (10n^2 + 66n + 116)\lambda^2 + O(\lambda^3)\right\}. \tag{3.17}$$

A list of values of λ versus $\bar\lambda$ for the case $n = 4$ is given in table 1. Furthermore, as for $n = 1$, improved convergence properties of the high-temperature expansion are obtained when the series are reexpanded in powers of a "character variable" v defined as in eqs.(I.6.14),(I.6.15), the ϕ-integrals now being n-dimensional.

Table 2: Comparision between estimates $(\kappa_c)_{HT}$ and $(\kappa_c)_{MC}$ of the critical hopping parameter for $n = 4$ as obtained from the high-temperature series analysis and various Monte-Carlo simulations

λ	$(\kappa_c)_{HT}$	$(\kappa_c)_{MC}$	ref.
1.000	0.2468(1)	0.2471(9)	[19]
3.202	0.2831(1)	0.2829(6)	[12]
∞	0.3041(1)	0.3039(8)	[19]
∞	0.3041(1)	0.3038(2)	[14]
∞	0.3041(1)	0.3045(7)	[15]

The analysis of the series for $n > 1$ is in no essential way different from the one applied earlier to the $n = 1$ series (see sect.6 of (I)), although now we have 4 more terms at our disposal and hence slightly improved error bounds in the final results. For example, for $n = 4$ we can extract the critical line $\kappa_c(\lambda)$ with an estimated relative error smaller than $2 \cdot 10^{-4}$ (see table 1). These values agree very well with earlier Monte-Carlo results, a comparision being given in table 2.

The series for m_R, g_R, Z_R and Z_R^O can be reliably evaluated in the range of κ which corresponds to correlation lengths m_R^{-1} less than about the mean extent in lattice spacings of the diagrams used in the high-temperature expansion. No Padé or other analytic extrapolation technique is needed here: one just monitors the apparent convergence of the first 14 partial sums and by comparing with the large order behaviour expected from the known singularities at the critical line, it is possible to obtain an estimate on the absolute deviation of the last partial sums from the exact value. In table 3 we give the results for the case $n = 4$ along the line $\kappa = 0.98\kappa_c$. Here the maximal correlation length attained (at $\bar{\lambda} = 1$) is less than 4. Finally we remark that for $\bar{\lambda} \leq 0.1$, the values of all quantities considered agree well with those obtained using leading orders bare perturbation theory.

Accurate Monte Carlo simulations of the O(4) model in the symmetric phase have recently been performed by Kuti et al.[11-13], using an effective action method. All of their data are at mass values $m_R \geq 0.27$ and we

Table 3: Values of m_R, g_R, Z_R and Z_R^O as calculated by the high-temperature expansion for $n = 4$ at a value of κ, given in column 2, which is equal to $0.98\kappa_c^*$, where κ_c^* is the estimate for κ_c given in table 1

$\bar{\lambda}$	κ	m_R	g_R	Z_R	Z_R^O
0.00	0.122500	0.404061(1)	0.0	4.081632(1)	0.015312(1)
0.01	0.123625	0.40123(8)	0.647(1)	4.044460(9)	0.01562(2)
0.02	0.124782	0.3985(2)	1.258(4)	4.00693(3)	0.01593(4)
0.03	0.125970	0.3959(2)	1.8371	3.96903(7)	0.01624(5)
0.04	0.127193	0.3935(3)	2.39(2)	3.9308(1)	0.01656(7)
0.05	0.128450	0.3911(4)	2.91(2)	3.8922(2)	0.01688(9)
0.06	0.129743	0.3888(4)	3.41(3)	3.8532(2)	0.0172(1)
0.07	0.131073	0.3865(5)	3.89(4)	3.8139(3)	0.0175(1)
0.08	0.132442	0.3844(5)	4.35(5)	3.7743(4)	0.0179(1)
0.09	0.133850	0.3823(6)	4.79(6)	3.7344(5)	0.0182(1)
0.10	0.135299	0.3802(6)	5.21(7)	3.6941(6)	0.0186(2)
0.20	0.152261	0.362(1)	8.7(2)	3.280(2)	0.0227(3)
0.30	0.174098	0.348(1)	11.2(3)	2.865(3)	0.0278(3)
0.40	0.199930	0.335(1)	13.1(5)	2.491(3)	0.0341(4)
0.50	0.226608	0.323(1)	14.7(6)	2.193(4)	0.0412(4)
0.60	0.250329	0.313(2)	15.9(7)	1.982(4)	0.0482(4)
0.70	0.268923	0.303(2)	16.9(8)	1.841(5)	0.0549(4)
0.80	0.282217	0.294(2)	17.7(9)	1.750(5)	0.0609(5)
0.90	0.291326	0.285(2)	18(1)	1.691(6)	0.0665(5)
1.00	0.298031	0.277(2)	19(1)	1.648(6)	0.0721(6)

can thus directly compare them with our results from the high-temperature series analysis (see table 4). The simulations were done on lattices of size L^4, where $L = 8$ for the first two points in table 4 and $L = 12$ for the other points. At $\lambda = \infty$, the coupling g_R was only measured on the smaller lattice with $L = 8$ and it is this value which we quote. In general, the agreement between the numerical data and our analytical work is rather good, but there are also some small discrepancies, which we cannot explain at the moment. However, one should keep in mind that the errors quoted for the Monte Carlo data are statistical only. Since these are rather small, it could be that systematic effects, e.g. those due to the finite extent of the lattice, are

Table 4: Comparison between numerical simulation data from refs.[11-13] (first line for given λ and κ) and the results of the high-temperature series analysis (second line).

λ	κ	m_R	g_R	Z_R
2.71414	0.260487	0.609(5)	27.4(5)	1.916(4)
2.71414	0.260487	0.600(1)	24.4(4)	1.905(2)
2.93996	0.271107	0.435(3)	22.1(5)	1.830(4)
2.93996	0.271107	0.416(2)	20.1(6)	1.826(4)
3.03359	0.275390	0.329(6)	19(1)	1.794(4)
3.03359	0.275390	0.325(2)	18.0(8)	1.796(5)
3.10505	0.278615	0.267(9)	16(1)	1.78(2)
3.10505	0.278615	0.242(2)	16(1)	1.773(6)
∞	0.2835	0.557(2)	25(4)	1.741(3)
∞	0.2835	0.559(1)	27.9(5)	1.740(3)
∞	0.2915	0.422(3)	22(2)	1.691(3)
∞	0.2915	0.419(2)	23.4(7)	1.689(4)

still significant. In any case, the observed agreement is impressive and this gives us confidence that our high-temperature analysis is correct, although at this point we cannot be absolutely sure that our error estimates are indeed realistic.

3.4 Tree-Level Unitarity Bound and Applicability of Renormalized Perturbation Theory

The tree-level unitarity bound on the renormalized coupling g_R is obtained as usual from the S-wave elastic scattering amplitude (cf. sect.7 of (I)). For general n, it reads

$$g_R < \frac{96\pi}{(n+2)\sqrt{3}}, \tag{3.18}$$

so that for the case of interest, $n = 4$, we have $g_R < 29$.

A non-trivial output of the high-temperature series analysis described in the previous subsection is that the renormalized coupling g_R at the maximal value of κ considered is already rather small. More precisely, at the boundary of the region in the phase diagram where we solve the theory by the high-temperature expansion ($\kappa = 0.98\kappa_c$ for $n = 4$), g_R is less than about 2/3 of the tree-level unitarity bound (cf. table 3). This property is necessary for our further procedure, because the integration of the renormalization group equations, which is started there and allows us to solve the theory in the remainder of the symmetric phase, is only practical if the initial value of g_R is in the perturbative range.

To further convince oneself of the applicability of perturbation theory for couplings satisfying the bound (3.18), one can calculate various quantities to two loops and compare successive terms. For example, for the true particle mass m defined through

$$\Gamma_R^{(2,0)}(p,-p)_{\alpha\beta} = 0, \qquad p = (im,0,0,0), \tag{3.19}$$

we have (neglecting scaling violations)

$$m = m_R\Big\{1 - 0.001287 \cdot \frac{1}{3}(n+2)\alpha_R^2 + O(g_R^3)\Big\}, \tag{3.20}$$

where

$$\alpha_R = g_R/16\pi^2. \tag{3.21}$$

For g_R less than the tree-level unitarity bound above the two-loop correction is small and m is practically equal to m_R. The O(n) scalar and tensor S-wave scattering lengths a_0^0 and a_0^2 are given by

$$\begin{aligned} a_0^0 &= -\frac{\pi}{6m_R}(n+2)\alpha_R\Big\{1 - \frac{1}{3}(n+2)\alpha_R \\ &\quad + (\frac{1}{9}n^2 + 0.34368\,n + 0.47219)\,\alpha_R^2 + O(g_R^3)\Big\}, \end{aligned} \tag{3.22}$$

$$\begin{aligned} a_0^2 &= -\frac{\pi}{3m_R}\alpha_R\Big\{1 - \frac{2}{3}\alpha_R \\ &\quad + (0.028066\,n + 0.47219)\,\alpha_R^2 + O(g_R^3)\Big\}, \end{aligned} \tag{3.23}$$

and as a final example we quote the connected 6-point function

$$\Gamma_R^{(6,0)}(0,\ldots,0)_{1\ldots1} + \frac{10}{m_R^2}\left(\Gamma_R^{(4,0)}(0,\ldots,0)_{1\ldots1}\right)^2 = \tag{3.24}$$
$$10\frac{g_R^2}{m_R^2}\Big\{1 - \frac{1}{36}(n+26)\alpha_R + \Big(0.13193\,(n-1) + \frac{9}{4}\Big)\alpha_R^2 + O(g_R^3)\Big\}.$$

In both the case of the scattering lengths and the 6-point coupling, the higher order corrections are not negligible, however the series still appear to be well-behaved when the coupling is less than 2/3 of the tree-level unitarity bound and in this respect the case $n = 4$ is in fact slightly more favourable than $n = 1$.

Incidentally we note that the scaling violations (the terms of order a^2, where a is the lattice spacing) which we neglected in the formulae above, are rather small, typically less than 10% of the continuum term, as soon as the correlation length is greater than about 2 lattice spacings. The region in the phase diagram where $m_R < 0.5$ will hence be referred to as the "scaling region".

3.5 Integration of the Renormalization Group Equations

To complete the analysis in the symmetric phase we integrate the renormalization group equations eqs.(I.4.26)-(I.4.29) using the results from the high-temperature expansion as initial conditions (i.e. the data along the line $\kappa = 0.98\kappa_c$ in the case $n = 4$). For the renormalization group functions β, γ and δ we use the 3-loop perturbative expressions (appropriate for our scheme) given in appendix A, and include full scaling violating effects to 1-loop order. The result of the integration for $n = 4$, together with the data obtained from the high-temperature series analysis in the range $0.3 \leq m_R \leq 1.0$, are given in table 5 at three representative values of $\bar{\lambda}$. The errors quoted are obtained by propagating the errors of the initial data. In particular, they do not include the uncertainties which arise from the fact that the β-function and the other renormalization group functions are only approximately known. This issue will later be discussed in greater detail (subsect.4.6). Here we only note that replacing the 3-loop formulae everywhere by the 2-loop expressions would not result in a significant change in the numbers listed in table 5, an exception being g_R at $\bar{\lambda} = 1$, where the two calculations only agree within the combined error margins at some points.

Table 5: Summary of results in the symmetric phase for $n = 4$ and $\bar{\lambda} = 0.01$, 0.1 and 1.0

$\bar{\lambda}$	m_R	g_R	Z_R	Z_R^O	κ
0.01	1.00	0.7982(3)	4.46321(4)	0.014076(2)	0.112027(1)
	0.90	0.7637(3)	4.36852(5)	0.014389(2)	0.114455(1)
	0.80	0.7332(4)	4.28375(5)	0.014683(4)	0.116720(1)
	0.70	0.7065(5)	4.20891(5)	0.014956(6)	0.118795(1)
	0.60	0.6834(7)	4.14399(5)	0.015204(9)	0.120656(1)
	0.50	0.6637(9)	4.08901(5)	0.01543(1)	0.122279(1)
	0.40	0.647(1)	4.04396(4)	0.01562(2)	0.123640(1)
	0.30	0.633(1)	4.00887(4)	0.01579(2)	0.124723(2)
	0.20	0.621(1)	3.98374(4)	0.01594(2)	0.125509(3)
	0.10	0.610(1)	3.96860(4)	0.01608(2)	0.125988(4)
	0.09	0.609(1)	3.96764(4)	0.01610(2)	0.126018(4)
	0.08	0.607(1)	3.96678(4)	0.01611(2)	0.126045(4)
	0.07	0.606(1)	3.96601(4)	0.01613(2)	0.126070(4)
	0.06	0.604(1)	3.96535(4)	0.01616(2)	0.126091(4)
	0.05	0.603(1)	3.96479(4)	0.01618(2)	0.126108(4)
	0.04	0.600(1)	3.96432(4)	0.01621(2)	0.126123(4)
	0.03	0.598(1)	3.96396(4)	0.01625(2)	0.126134(4)
	0.02	0.594(1)	3.96370(4)	0.01630(2)	0.126143(4)
	0.01	0.588(1)	3.96353(4)	0.01638(2)	0.126148(4)
0.10	1.00	7.16(2)	4.1088(4)	0.01596(1)	0.121673(8)
	0.90	6.77(2)	4.1079(4)	0.01639(2)	0.124421(9)
	0.80	6.42(3)	3.9363(5)	0.01683(3)	0.12700(1)
	0.70	6.09(4)	3.8637(6)	0.01725(4)	0.12938(1)
	0.60	5.80(4)	3.8005(7)	0.01767(7)	0.13153(1)
	0.50	5.52(6)	3.7465(8)	0.0181(1)	0.13342(1)
	0.40	5.26(7)	3.7018(8)	0.0185(1)	0.13502(1)
	0.30	4.99(7)	3.6668(9)	0.0190(2)	0.13631(2)
	0.20	4.71(6)	3.6412(9)	0.0195(2)	0.13726(2)
	0.10	4.33(5)	3.6251(9)	0.0204(2)	0.13786(3)
	0.09	4.28(5)	3.6240(9)	0.0205(2)	0.13789(3)
	0.08	4.23(5)	3.6230(9)	0.0206(2)	0.13793(3)
	0.07	4.17(5)	3.6221(9)	0.0208(2)	0.13796(3)
	0.06	4.11(5)	3.6213(9)	0.0209(2)	0.13799(3)
	0.05	4.03(5)	3.621(1)	0.0211(2)	0.13801(3)
	0.04	3.95(5)	3.620(1)	0.0214(2)	0.13803(3)
	0.03	3.84(4)	3.619(1)	0.0217(2)	0.13804(3)
	0.02	3.70(4)	3.619(1)	0.0221(2)	0.13806(3)
	0.01	3.48(4)	3.618(1)	0.0228(2)	0.13806(3)

Table 5: (continued)

$\bar{\lambda}$	m_R	g_R	Z_R	$Z_R^{\mathcal{O}}$	κ
1.00	1.00	44.2(2)	1.967(1)	0.04568(3)	0.25223(4)
	0.90	40.1(2)	1.907(1)	0.04827(4)	0.25984(5)
	0.80	36.2(3)	1.852(1)	0.05107(6)	0.26723(6)
	0.70	32.6(4)	1.802(2)	0.0541(1)	0.27430(7)
	0.60	29.2(5)	1.757(3)	0.0575(2)	0.28094(8)
	0.50	26.0(6)	1.717(4)	0.0613(2)	0.28705(8)
	0.40	22.8(8)	1.682(5)	0.0656(4)	0.29247(8)
	0.30	20(1)	1.653(6)	0.0707(6)	0.29708(7)
	0.20	16.4(9)	1.634(7)	0.077(1)	0.30072(9)
	0.10	12.9(6)	1.622(7)	0.088(2)	0.3031(1)
	0.09	12.5(5)	1.621(7)	0.089(2)	0.3033(1)
	0.08	12.1(5)	1.620(7)	0.091(2)	0.3035(1)
	0.07	11.7(5)	1.619(7)	0.093(2)	0.3036(1)
	0.06	11.2(4)	1.618(7)	0.095(2)	0.3037(1)
	0.05	10.7(4)	1.617(7)	0.097(2)	0.3038(1)
	0.04	10.2(3)	1.616(8)	0.100(2)	0.3039(1)
	0.03	9.5(3)	1.615(8)	0.103(2)	0.3040(1)
	0.02	8.7(3)	1.615(8)	0.108(3)	0.3040(1)
	0.01	7.7(2)	1.613(8)	0.116(3)	0.3041(1)

An important insight gained from our calculations is that the qualitative behaviour of the model in the symmetric phase does apparently not depend very much on n. In particular, the detailed results obtained for $n = 1$, $n = 4$ and $n = \infty$ (a case which is known to be exactly soluble for a long time) show that the renormalized coupling is always smaller than about 2/3 of the tree-level unitarity bound in the range of bare parameters where the correlation length m_R^{-1} is greater than 2 or 3 lattice spacings. Furthermore, the renormalization group trajectories (curves of constant g_R) in the plane of bare parameters all end at the line $\lambda = \infty$, the ultra-violet cutoff being maximal there. The triviality bound on g_R is thus saturated in the σ-model limit. A quantitative plot of the flow of the renormalization group trajectories for $n = 4$ will be shown later on (subsect.4.6) when the analysis of the broken symmetry phase is completed. Finally note that the wave function renormalization constant $Z_R' = 2\kappa Z_R$ of the canonically normalized bare field $\phi_a' = \sqrt{2\kappa}\phi_a$ is a number close to 1 at all points quoted in table 5, a fact which we have already observed earlier in the case $n = 1$.

Table 6: Comparison between results for $n = 4, \lambda = \infty$, obtained from the high-temperature analysis (first row for a given m_R) and from the integration of the renormalization group equations (second row) with initial values equated to the high-temperature data at $m_R = 0.28$

m_R	g_R	Z_R	$Z_R^{\mathcal{O}}$	κ
0.50	26.0(6)	1.717(4)	0.0613(2)	0.28705(8)
0.50	27(2)	1.705(9)	0.061(1)	0.2870(2)
0.40	22.8(8)	1.682(5)	0.0656(4)	0.29247(8)
0.40	23(2)	1.676(8)	0.065(1)	0.2925(1)
0.30	20(1)	1.653(6)	0.0707(6)	0.29708(7)
0.30	20(1)	1.652(7)	0.0707(7)	0.29708(7)
0.20	16(1)	1.631(7)	0.077(1)	0.30071(5)
0.20	16.4(9)	1.634(7)	0.077(1)	0.30072(9)
0.10	12(2)	1.616(8)	0.088(2)	0.30315(2)
0.10	12.9(6)	1.622(7)	0.088(2)	0.3031(1)

In a neighborhood of the boundary of the scaling region (i.e. near the line $\kappa = 0.98\kappa_c$ in the case $n = 4$), both methods of calculation, the high-temperature expansion and the renormalization group equations apply and can hence be compared. This provides an important check on the crucial step in our procedure, which is the matching between the high-temperature curves and the weak coupling scaling behaviour. As an example, the result of such a comparison is shown in table 6 for the case $n = 4, \lambda = \infty$. The matching is truly impressive and it is obvious from this test, that the choice of the point where to start the integration of the renormalization group equations is of little import to the final results. The same is true for the smaller values of λ, the matching being even more accurate there.

It is worth mentioning at this point that our analysis of the $n = 4$ model looks in fact more stable than our earlier treatment of the one-component

model. The reason for this is two-fold. First, the high-temperature series used here is longer and hence the errors on the final numbers tend to be smaller. In addition, the high-temperature series analysis can be pushed to larger correlation lengths, i.e. deeper into the scaling region, so that the matching with the renormalization group analysis is somewhat easier. Secondly, in our renormalization scheme, the β-function has only one (universal) term in the large n limit, and it is therefore no surprise that its perturbation expansion is better behaved for $n = 4$ than for $n = 1$. In particular, the one-loop term clearly dominates in the whole integration region and the difference between the 2-loop and the 3-loop results is diminished. In any case, the qualitative assumptions underlying our analysis remain the same as in the one-component model and further numerical studies of the O(4) theory in the symmetric phase should therefore be made in order to obtain an independent check on our results [1].

In table 7 we finally list the integration constants C_i defined through eqs.(3.5)-(3.7). They were obtained by the method described in (II), subsect.4.4, using the 3-loop expressions for the renormalization group functions (as above). The errors only include the uncertainties originating from the high-temperature series analysis. The agreement with the perturbative formula

$$\ln C_1(\bar{\lambda}) = \frac{\pi^2}{16\bar{\lambda}} - \frac{13}{24}\ln\bar{\lambda} + 0.69604 + O(\bar{\lambda}), \qquad (3.25)$$

is excellent up to about $\bar{\lambda} = 0.3$ and the corresponding expressions for C_2 and C_3 also reproduce the values quoted in table 7 up to about $\bar{\lambda} = 0.1$.

4. Analysis in the Broken Symmetry Phase

In this section we describe the analysis in the Goldstone phase and initially consider the theory for non-vanishing external field h (cf. eq.(2.1)). For the field $\phi_a(x)$ we introduce the familiar notation [2]

$$\pi_a(x) \;=\; \phi_a(x), \qquad (a = 1, ..., n-1), \qquad (4.1)$$

[1] The existing data of Kuti et al.[11-13] are all in the range of κ, where the high-temperature expansion applies (cf. subsect.3.3). For a significant comparision with the results of the integration of the renormalization group equations, one would have to perform accurate simulations at $m_R \leq 0.2$. This is clearly very demanding, especially if one wants to make sure that the finite size effects are under control.

[2] In the following Greek indices $\alpha, \beta, ..$ run from $1, ..., n$ and Latin indices $a, b, ..$, from $1, ..., n-1$.

Table 7: Values of $\ln C_i(\lambda)$ versus $\bar{\lambda}$ for $n = 4$

$\bar{\lambda}$	$\ln C_1(\lambda)$	$\ln C_2(\lambda)$	$\ln C_3(\lambda)$
0.01	64.8(1)	1.37681(1)	−4.375(2)
0.02	33.6(1)	1.36718(3)	−4.021(4)
0.03	23.1(1)	1.35739(5)	−3.810(6)
0.04	17.8(1)	1.34743(8)	−3.658(8)
0.05	14.6(1)	1.3373(1)	−3.538(9)
0.06	12.5(1)	1.3270(1)	−3.44(1)
0.07	10.9(1)	1.3165(2)	−3.35(1)
0.08	9.7(1)	1.3059(2)	−3.27(1)
0.09	8.8(1)	1.2950(2)	−3.21(1)
0.10	8.1(1)	1.2840(3)	−3.14(2)
0.20	4.6(1)	1.1635(8)	−2.68(2)
0.30	3.4(1)	1.027(1)	−2.34(3)
0.40	2.8(1)	0.887(2)	−2.05(3)
0.50	2.4(1)	0.759(2)	−1.80(3)
0.60	2.1(1)	0.658(3)	−1.60(3)
0.70	1.9(1)	0.584(4)	−1.44(3)
0.80	1.8(1)	0.533(4)	−1.31(4)
0.90	1.6(1)	0.499(4)	−1.20(4)
1.00	1.5(1)	0.474(5)	−1.11(4)

$$\sigma(x) \;=\; \phi_n(x). \qquad (4.2)$$

For the discussion of renormalization and also in explicit perturbative calculations, an important rôle is played by the O(n) Ward identities. We thus start by deriving them and then go on to describe the perturbative analysis, ending up with the integration of the renormalization group equations with initial data given along the critical line.

4.1 Ward Identities

The vertex functions $\Gamma^{(k,l)}(p_1, ..., q_l)_{a_1 ... a_k}$ defined in sect.2 are now only invariant under O($n-1$) rotations of the π-field. Using the invariance of the measure in eq.(2.4) under "chiral" rotations

$$\delta_a \sigma \;=\; \pi_a, \qquad (4.3)$$

$$\delta_a \pi_b = -\delta_{ab}\sigma, \tag{4.4}$$

the generating functional W can be shown to satisfy

$$\sum_x \left\{ (h + H_n(x)) \frac{\partial}{\partial H_a(x)} - H_a(x) \frac{\partial}{\partial H_n(x)} \right\} W[H,K] = 0. \tag{4.5}$$

For the vertex functional one then derives the identity

$$\sum_x \left\{ (v + M_n(x)) \frac{\partial}{\partial M_a(x)} - M_a(x) \frac{\partial}{\partial M_n(x)} \right\} \Gamma[M,K] = -h \sum_x M_a(x). \tag{4.6}$$

Written explicitly in terms of the vertex functions one has

$$v\Gamma^{(2,0)}(0,0)_{ab} = -h\delta_{ab}, \tag{4.7}$$

$$v\Gamma^{(k+1,l)}(0,p_1,\ldots,p_k;q_1,\ldots,q_l)_{a\alpha_1\ldots\alpha_k} = \tag{4.8}$$
$$\sum_{j=1}^{k}\sum_{\beta=1}^{n} \Gamma^{(k,l)}(p_1,\ldots,p_k;q_1,\ldots,q_l)_{\alpha_1\ldots\alpha_{j-1}\beta\alpha_{j+1}\ldots\alpha_k}(\delta_{\beta n}\delta_{a\alpha_j} - \delta_{\beta a}\delta_{n\alpha_j}),$$

where $k \geq 1$, $k+l \geq 2$ and v denotes the vacuum expectation value of σ (cf. eq.(2.6)).

An immediate consequence of eq.(4.7) is the Goldstone theorem: when there is spontaneous symmetry breaking in the limit $h = 0$, the vacuum expectation value of the field does not vanish and hence $\Gamma^{(2,0)}(0,0)_{ab} = 0$, i.e. there are $n-1$ Goldstone bosons. Another less obvious use of the Ward identities is in the proof of the (perturbative) renormalizability of the model [25], where they allow one to show that all divergences can be subtracted simply by renormalizing the parameters in the action and by rescaling the fields ϕ_a and $\mathcal{O}$ as in the symmetric phase. In particular, the Ward identities (4.7) and (4.8) are also satisfied, with a renormalized v and h, by the renormalized vertex functions introduced below.

4.2 Perturbation Theory

In perturbation theory one expands the functional integral (2.4) around the constant field

$$\phi_a = \delta_{an} s_0, \tag{4.9}$$

where s_0 is chosen such as to minimize the action S_h, i.e. s_0 is the positive root of

$$4\lambda s_0^3 + 2(1 - 8\kappa - 2\lambda)s_0 - h = 0. \tag{4.10}$$

In terms of the fluctuation fields φ_0, π_0 and σ_0 defined by

$$(\varphi_0)_\alpha = \sqrt{2\kappa}(\phi_\alpha - \delta_{n\alpha}s_0), \tag{4.11}$$
$$(\pi_0)_a = (\varphi_0)_a, \tag{4.12}$$
$$\sigma_0 = (\varphi_0)_n, \tag{4.13}$$

the action becomes (up to a constant)

$$S_h = \sum_x \Big\{ \frac{1}{2}\sum_{\mu=0}^{3} \partial_\mu\varphi_0 \cdot \partial_\mu\varphi_0 + \frac{1}{2}\mu_0^2 \pi_0 \cdot \pi_0 + \frac{1}{2}m_0^2\sigma_0^2 + \frac{1}{3!}\sqrt{3g_0(m_0^2 - \mu_0^2)}(\varphi_0 \cdot \varphi_0)\,\sigma_0 + \frac{g_0}{4!}(\varphi_0 \cdot \varphi_0)^2 \Big\}, \tag{4.14}$$

where the parameters μ_0, m_0 and g_0 are given by

$$\mu_0^2 = (1 - 8\kappa - 2\lambda + 2\lambda s_0^2)/\kappa, \tag{4.15}$$
$$m_0^2 = (1 - 8\kappa - 2\lambda + 6\lambda s_0^2)/\kappa, \tag{4.16}$$
$$g_0 = 6\lambda/\kappa^2. \tag{4.17}$$

In perturbation theory, μ_0, m_0 and g_0 are regarded as the independent bare parameters, while h, κ and λ are to be expressed in terms of them by solving eqs.(4.10) and (4.15)-(4.17). Note that the limit $\mu_0 \to 0$ implies $h \to 0$, i.e. this is the case we are ultimately interested in.

Next we introduce the composite operator $\mathcal{O}_0$ as in eq.(2.3) with ϕ replaced by φ_0 and bare vertex functions $\Gamma_0^{(k,l)}$ of φ_0 and $\mathcal{O}_0$ analogously to $\Gamma^{(k,l)}$ (cf. eqs.(2.4)-(2.9)). The relation between these two sets of vertex functions is

$$\Gamma^{(k,l)} = (2\kappa)^{k/2-l}\Gamma_0^{(k,l)} \qquad \text{for } (k,l) \neq (0,1),(1,1), \tag{4.18}$$
$$\Gamma^{(0,1)} = (2\kappa)^{-1}\Gamma_0^{(0,1)} + (2\kappa)^{-1/2}16v_0s_0 + 8s_0^2, \tag{4.19}$$
$$\Gamma^{(1,1)}(p;q)_\alpha = (2\kappa)^{-1/2}\Gamma_0^{(1,1)}(p;q)_\alpha + \delta_{\alpha n}2s_0\sum_{\mu=0}^{3}(1 + \cos p_\mu). \tag{4.20}$$

In the above, v_0 is the vacuum expectation value of σ_0 which is related to v through

$$v = (2\kappa)^{-1/2} v_0 + s_0. \tag{4.21}$$

The bare perturbation expansion of the vertex functions $\Gamma_0^{(k,l)}$ (and hence of $\Gamma^{(k,l)}$) in powers of g_0 is now easily derived from the action (4.14). In particular, at tree-level the non-vanishing vertex functions are

$$\Gamma^{(2,0)}(p,-p)_{ab} = -\delta_{ab}\, 2\kappa\,(\mu_0^2 + \hat{p}^2), \tag{4.22}$$

$$\Gamma^{(2,0)}(p,-p)_{nn} = -2\kappa\,(m_0^2 + \hat{p}^2), \tag{4.23}$$

$$\Gamma^{(3,0)}_{\alpha\beta\gamma} = -\frac{1}{3} C_4(\alpha,\beta,\gamma,n)(2\kappa)^{3/2}\sqrt{3g_0(m_0^2-\mu_0^2)}, \tag{4.24}$$

$$\Gamma^{(4,0)}_{\alpha\beta\gamma\delta} = -\frac{1}{3} C_4(\alpha,\beta,\gamma,\delta)(2\kappa)^2 g_0, \tag{4.25}$$

$$\Gamma^{(0,1)} = 8v^2, \tag{4.26}$$

$$\Gamma^{(1,1)}(p;q)_\alpha = \delta_{\alpha n} v(16 - \hat{q}^2), \tag{4.27}$$

$$\Gamma^{(2,1)}(p_1,p_2;q)_{\alpha\beta} = \delta_{\alpha\beta}(16 - \hat{p}_1^2 - \hat{p}_2^2), \tag{4.28}$$

where $\hat{p}^2$ is given by eq.(II.2.26). Furthermore, we have

$$v = s_0 + O(\sqrt{g_0}), \tag{4.29}$$

and one may readily verify that the Ward identities (4.7) and (4.8) are satisfied to lowest order.

4.3 Renormalization Conditions

In the broken symmetry phase for $n > 1$ one cannot impose all renormalization conditions at zero momentum due to infra-red divergences. We here adopt the following renormalization scheme. The wave function renormalization constant Z_R and the "pion" mass μ_R are defined through the behaviour of the negative inverse π-propagator at zero momentum, viz.

$$\Gamma^{(2,0)}(p,-p)_{ab} = -\delta_{ab} Z_R^{-1}\{\mu_R^2 + p^2 + O(p^4)\}, \qquad (p \to 0). \tag{4.30}$$

The vacuum expectation value v_R of the renormalized σ-meson field is then given by

$$v_R = v Z_R^{-1/2}, \tag{4.31}$$

and a renormalized magnetic field h_R may be introduced through

$$h_R = h Z_R^{1/2}. \tag{4.32}$$

How to define a renormalized σ-mass m_R is less obvious, because the σ-particle is unstable (it decays into any even number of Goldstone bosons). In particular, in the limit $h = 0$, the σ-propagator is singular at zero momentum and the definition (II.2.27) of m_R employed in the case $n = 1$ can therefore not be taken over. A non-singular definition which we found convenient for our calculations, is specified by

$$\mathrm{Re}\left\{\Gamma^{(2,0)}(p,-p)_{nn}\Big|_{p=\bar{p}}\right\} = 0, \tag{4.33}$$

where

$$\bar{p} = (im_R, 0, 0, 0) \tag{4.34}$$

and the zero of the σ-meson propagator closest to the origin $p = 0$ should be taken. The relation of m_R to the physical mass m_σ of the σ-resonance is discussed below.

Finally, a renormalized Higgs self-coupling g_R may be defined through

$$g_R = 3(m_R^2 - \mu_R^2)/v_R^2, \tag{4.35}$$

and the wave function renormalization constant $Z_R^{\mathcal{O}}$ of the composite operator $\mathcal{O}$ is determined by

$$\mathrm{Re}\left\{\Gamma^{(1,1)}(p,-p)_n\Big|_{p=\bar{p}}\right\} = v\,(Z_R Z_R^{\mathcal{O}})^{-1}. \tag{4.36}$$

This is convenient from a computational point of view since the perturbative graphs needed in the evaluation of $Z_R^{\mathcal{O}}$ then resemble those required for the determination of m_R. Note that to lowest order perturbation theory, we have

$$m_R = \mathrm{acosh}\left(1 + \frac{1}{2}m_0^2\right), \tag{4.37}$$

$$g_R = g_0(m_R^2 - \mu_0^2)/(m_0^2 - \mu_0^2), \tag{4.38}$$

i.e. the renormalized σ-mass and the coupling are equal to their bare equivalents only up to scaling violation terms.

Having introduced the renormalized parameters and the wave function renormalization constants, renormalized vertex functions $\Gamma_R^{(k,l)}$ may be introduced in the usual way (see e.g. eqs.(II.2.33)-(II.2.35)), a little difference being that the additive subtraction of $\Gamma^{(0,2)}$ is made at $q = \bar{p}$ rather than at zero momentum. The renormalized vertex functions are considered to be functions of the momenta and the parameters μ_R, m_R and g_R. Note that v_R and h_R are simple combinations of these parameters, v_R being determined through eq.(4.35) and h_R by

$$h_R = v_R \mu_R^2, \tag{4.39}$$

which is a consequence of the Ward identity (4.7) and the definition of the quantities involved.

4.4 Tree-level Unitary Bound and Results from Renormalized Perturbation Theory

The S-wave "isospin" 0 channel partial wave amplitude of elastic scattering of the Goldstone bosons is, neglecting scaling violations, to tree-level given by

$$t_0^0 = \frac{g_R}{48\pi\sqrt{s}} \left\{ (n-1)\frac{s}{m_R^2 - s} - 2 + 2\frac{m_R^2}{s} \ln(1 + \frac{s}{m_R^2}) \right\}, \tag{4.40}$$

where s is the total center-of-mass energy squared. This representation is obviously only valid outside the resonance region, i.e. when $|s - m_R^2| \gg m_R \Gamma_\sigma$, Γ_σ being the width of the σ-meson (see eqs.(4.43),(4.45) below). If we now impose the unitarity requirement

$$\left| \mathrm{Re}(t_0^0) \right| < 1/\sqrt{s} \tag{4.41}$$

at large s, the bound

$$g_R < \frac{48\pi}{n+1} \tag{4.42}$$

is obtained. For the case $n = 4$ this implies $g_R < 30$, which is practically the same bound as in the symmetric phase (cf. subsect. 3.4). We also note that this is about half the value quoted by Lee, Quigg and Thacker [23] in their study of the large Higgs mass limit of the Standard Model, the reason for this discrepancy being that these authors only impose the unitarity restriction $|t_0^0| < 2/\sqrt{s}$ instead of the stronger requirement eq.(4.41) (an additional factor of $\frac{5}{6}$ arises from the fact that in ref.[23] also Higgs production is included in the unitarity balance).

The physical σ-meson mass m_σ and width Γ_σ are defined through the position of the pole on the second sheet of the analytically continued σ-meson propagator, viz.

$$\Gamma^{(2,0)}(p,-p)_{nn}\Big|_{p=(im_\sigma + \frac{1}{2}\Gamma_\sigma, 0, 0, 0)} = 0. \tag{4.43}$$

For weak coupling, the renormalized mass m_R defined in eq.(4.33) and the physical mass m_σ are numerically very close; to 2-loop renormalized perturbation theory, with $\mu_R = 0$, they are related by [1]

$$m_\sigma = m_R \left\{ 1 + \frac{\pi^2}{288}(n-1)^2 \alpha_R^2 + O(g_R^3) \right\}. \tag{4.44}$$

For the σ-meson width Γ_σ, including the one-loop correction, we find

$$\frac{\Gamma_\sigma}{m_\sigma} = \frac{\pi}{6}(n-1)\alpha_R \left\{ 1 + (\frac{n}{6} - \pi\sqrt{3} + \frac{15}{6} + \frac{5}{18}\pi^2)\alpha_R + O(g_R^2) \right\}. \tag{4.45}$$

This result was obtained by calculating the σ-propagator to 2-loops and determining the pole as specified in eq.(4.43). For the special case $n = 4$, eq.(4.45) is in complete agreement with a formula published recently by Marciano and Willenbrock [24]. Note that for couplings g_R which are less than $\frac{2}{3}$ of the tree-level unitarity bound, the σ-resonance is still relatively narrow, i.e. its width is less than about 20% of its mass. Furthermore, the one-loop correction to Γ_σ happens to be very small in this range of couplings.

4.5 Callan-Symanzik Equation and Scaling Laws

The Callan-Symanzik equation for non-vanishing external "magnetic" field h is derived in essentially the same way as for the one-component model without "magnetic" field (cf. subsect.4.3 of (I)). A notable difference is perhaps that here we need two equations for the bare vertex functions to start with, because there are two renormalized mass parameters. One set of equations derives from

$$\frac{\partial S_h}{\partial \kappa} = -\sum_x \mathcal{O}(x) \tag{4.46}$$

as before, while a second set of relations between the bare vertex functions is obtained from

$$\frac{\partial S_h}{\partial h} = -\sum_x \sigma(x). \tag{4.47}$$

[1] We would here like to take the opportunity to correct an error in (II): eq.(II.5.2) should read $m = m_R\{1 - 0.01465\alpha_R - 0.03971\alpha_R^2 + O(g_R^3)\}$.

When expressed in terms of the renormalized vertex functions, these relations can be combined to yield the Callan-Symanzik equation which may be written in the form [1]

$$\left\{\mu_R\frac{\partial}{\partial\mu_R}+m_R\frac{\partial}{\partial m_R}+\beta\frac{\partial}{\partial g_R}-k\gamma-l\delta\right\}\Gamma_R^{(k,l)}= \tag{4.48}$$

$$\vartheta m_R\,\Gamma_R^{(k+1,l)}\Big|_{p_{k+1}=0,\alpha_{k+1}=n}+\epsilon m_R^2\,\Gamma_R^{(k,l+1)}\Big|_{q_{l+1}=0}+\delta_{k1}\delta_{l0}\delta_{\alpha_1 n}\omega m_R^3.$$

The Callan-Symanzik coefficients β, γ, etc. are functions of μ_R, m_R and g_R which, in the scaling region, only depend on the coupling and the mass ratio

$$r=\frac{\mu_R}{m_R}. \tag{4.49}$$

At fixed bare coupling λ, the condition $r=$ constant defines a curve $h=h(\kappa)$ in the plane of bare parameters h,κ which passes through the critical point $h=0,\kappa=\kappa_c$. Along these curves the renormalization group functions β,γ,δ and ϵ are given by the usual relations eqs.(I.4.21)-(I.4.24) while ϑ is determined by eq.(II.3.3). The new coefficient ω, which multiplies the last term in eq.(4.48), is given by

$$\omega=Z_R^{1/2}\left(\frac{\partial h}{\partial\kappa}\right)\left(m_R^2\frac{\partial m_R}{\partial\kappa}\right)^{-1} \tag{4.50}$$

(derivatives with respect to κ are at fixed λ and r).

Using our renormalization conventions and the Ward identities, ϑ and ω can be shown to be related to the other Callan-Symanzik coefficients through

$$\vartheta = \left(1+\gamma-\frac{\beta}{2g_R}\right)\sqrt{3(1-r^2)/g_R}, \tag{4.51}$$

$$\omega = r^2\left(3-\gamma-\frac{\beta}{2g_R}\right)\sqrt{3(1-r^2)/g_R}. \tag{4.52}$$

Note, however, that contrary to the situation in our previous treatment of the $n=1$ case, there is unfortunately no simple relation of ϵ to the other functions here, because the renormalized mass m_R and the normalization constant Z_R^O were defined at a non-zero momentum.

The renormalization group functions govern the scaling behaviour of μ_R, m_R, etc. when the critical line is approached at fixed λ and r. Since these

[1] Eq.(4.48) is valid for all $k\geq 1$ and all $l\geq 0$.

quantities were defined infra-red singularity free, we expect that β, γ, δ and ϵ remain well-defined in the absence of the symmetry breaking term, i.e when $h=r=0$, and this is indeed what we find in our explicit calculations. The renormalization group functions for $r=0$, appropriate to our renormalization conventions, are listed in appendix B for general n up to 3-loops.

By solving the renormalization group equations close to the critical line, we may now derive scaling laws as in the symmetric phase (cf. subsect.3.2). For vanishing external field h, they read

$$m_R = C_1'(\beta_1 g_R)^{-\beta_2/\beta_1^2}e^{-1/\beta_1 g_R}\{1+O(g_R)\}, \tag{4.53}$$

$$Z_R = C_2'\{1+O(g_R)\}, \tag{4.54}$$

$$Z_R^O = C_3'(g_R)^{\delta_1/\beta_1}\{1+O(g_R)\}, \tag{4.55}$$

$$\kappa-\kappa_c = \frac{1}{2}C_3'm_R^2(g_R)^{\delta_1/\beta_1}\{1+O(g_R)\}, \tag{4.56}$$

where the integration constants C_i' depend on λ. Note that there is an extra factor of $-\frac{1}{2}$ in eq.(4.56) as compared to the corresponding scaling law in the symmetric phase. Finally, we mention that as a simple consequence of the above relations, the vacuum expectation value v of ϕ goes to zero as one approaches the critical line according to

$$v \underset{\tau\to 0}{\propto} (-\tau)^{1/2}\,|\ln(-\tau)|^{\frac{3}{n+8}}, \tag{4.57}$$

where $\tau=1-\kappa/\kappa_c$.

As discussed in great detail in sect.4 of (II), the integration constants $C_i(\lambda)$ and $C_i'(\lambda)$ can be related to each other by reconstructing the theory on both sides of the critical line in terms of the critical theory using mass perturbation theory. This calculation only requires the computation of the renormalization constants in both phases to one-loop bare perturbation theory and, with the help of appendix C, the result

$$C_1'(\lambda)=C_1(\lambda)\,\exp\left\{(2n+17-3\sqrt{3\pi})/(2n+16)\right\}, \tag{4.58}$$

$$C_i'(\lambda)=C_i(\lambda), \qquad (i=2,3), \tag{4.59}$$

is quickly obtained. In particular, for $n=4$ we have

$$C_1'(\lambda)=1.435\cdot C_1(\lambda). \tag{4.60}$$

Note that eq.(4.58) does not reduce to eq.(II.4.37) for $n = 1$, because we here use a different renormalization scheme in the broken symmetry phase. For $n \to \infty$, on the other hand, the relations (4.58), (4.59) can readily be verified from the exact solution.

4.6 Integration of the Renormalization Group Equations

With the integration constants C_i' determined through the relations supplied in the previous subsection, we can now integrate the renormalization group equations away from the critical line into the broken symmetry phase. This is continued until g_R becomes so large that the applicability of the perturbative formulae for the renormalization group functions becomes doubtful. From our previous experience we expect the approximation to be under control while g_R stays below $\frac{2}{3}$ of the tree-level unitarity bound eq.(4.42). In table 8 we give the results of this analysis for the O(4)-model for three values of $\bar{\lambda}$, using 3-loop renormalization group functions appropriate for our renormalization scheme and including cutoff effects to 1-loop order (appendix B). The errors quoted are obtained by propagating the estimated errors on $C_i(\lambda)$ as given in table 7 [1].

An important result of the integration of the renormalization group equations in the Goldstone phase of the $n = 4$ model is that the coupling g_R apparently does not exceed a value of about 20 as long as the ultra-violet cutoff Λ is greater than 2 times the σ-mass. In particular, the use of the perturbative formulae for the Callan-Symanzik coefficients in this region of the phase diagram is justified *a posteriori* (recall the tree-level unitarity bound $g_R < 29$).

The physical picture of the O(4) model thus obtained is practically the same as for the one-component model treated in our earlier papers. In particular, the flow of the renormalization group trajectories (lines of constant g_R) in the (κ, λ)-plane looks very similiar for the two cases (see fig.1 below and fig.2 of (II), respectively). The minimal value of m_R along these trajectories is always attained in the limit $\lambda \to \infty$. For small values of the ultra-violet cutoff Λ, the maximal possible value of g_R is thus given by the entries for

[1] The results at $\lambda = \infty$ have already been published in ref.[5]. Unfortunately, some of the errors quoted there are a little too small due to inaccurate rounding in the error propagation subroutine.

Table 8: Summary of results in the Goldstone phase for $n = 4$ and $\bar{\lambda} = 0.01$, 0.1 and 1.0

$\bar{\lambda}$	m_R	g_R	Z_R	Z_R^O	κ
0.01	0.50	0.590(1)	3.89734(4)	0.01598(5)	0.12821(3)
	0.40	0.598(1)	3.92048(4)	0.01601(5)	0.12745(3)
	0.30	0.604(1)	3.93827(4)	0.01605(5)	0.12688(3)
	0.20	0.606(1)	3.95090(4)	0.01610(5)	0.12647(3)
	0.10	0.604(1)	3.95846(4)	0.01618(5)	0.12623(3)
	0.09	0.603(1)	3.95894(4)	0.01620(5)	0.12621(3)
	0.08	0.602(1)	3.95937(4)	0.01621(5)	0.12620(3)
	0.07	0.601(1)	3.95975(4)	0.01623(5)	0.12619(3)
	0.06	0.600(1)	3.96008(4)	0.01625(5)	0.12618(3)
	0.05	0.598(1)	3.96036(4)	0.01627(5)	0.12617(3)
	0.04	0.596(1)	3.96059(4)	0.01630(5)	0.12616(3)
	0.03	0.594(1)	3.96077(4)	0.01633(5)	0.12616(3)
	0.02	0.590(1)	3.96091(4)	0.01638(5)	0.12615(3)
	0.01	0.584(1)	3.96100(4)	0.01647(5)	0.12615(3)
0.10	0.50	4.79(7)	3.541(1)	0.0193(4)	0.14048(8)
	0.40	4.72(7)	3.563(1)	0.0196(4)	0.13961(6)
	0.30	4.61(6)	3.580(1)	0.0200(5)	0.13894(5)
	0.20	4.43(6)	3.593(1)	0.0204(5)	0.13846(4)
	0.10	4.14(5)	3.600(1)	0.0212(5)	0.13816(3)
	0.09	4.10(5)	3.601(1)	0.0213(5)	0.13814(3)
	0.08	4.05(5)	3.602(1)	0.0214(5)	0.13813(3)
	0.07	4.00(5)	3.602(1)	0.0215(5)	0.13811(3)
	0.06	3.94(5)	3.602(1)	0.0217(5)	0.13810(3)
	0.05	3.88(4)	3.603(1)	0.0219(5)	0.13809(3)
	0.04	3.80(4)	3.603(1)	0.0221(5)	0.13808(3)
	0.03	3.70(4)	3.604(1)	0.0224(5)	0.13807(3)
	0.02	3.57(4)	3.604(1)	0.0228(5)	0.13806(3)
	0.01	3.37(3)	3.605(1)	0.0235(5)	0.13806(3)

Table 8: (continued)

$\bar{\lambda}$	m_R	g_R	Z_R	Z_R^O	κ
1.00	0.50	19(1)	1.559(9)	0.078(5)	0.3130(7)
	0.40	17(1)	1.571(9)	0.081(5)	0.3101(5)
	0.30	15.6(8)	1.581(8)	0.085(5)	0.3077(3)
	0.20	13.6(6)	1.589(8)	0.091(5)	0.3058(2)
	0.10	11.3(4)	1.595(8)	0.099(6)	0.30458(9)
	0.09	11.0(4)	1.595(8)	0.100(6)	0.30450(8)
	0.08	10.7(4)	1.596(8)	0.102(6)	0.30442(8)
	0.07	10.3(3)	1.596(8)	0.103(6)	0.30435(7)
	0.06	10.0(3)	1.597(8)	0.105(6)	0.30429(7)
	0.05	9.6(3)	1.597(8)	0.107(6)	0.30424(7)
	0.04	9.1(3)	1.598(8)	0.110(6)	0.30420(7)
	0.03	8.6(2)	1.598(8)	0.113(6)	0.30416(6)
	0.02	8.0(2)	1.599(8)	0.117(6)	0.30414(6)
	0.01	7.1(2)	1.600(8)	0.124(6)	0.30412(6)

$\bar{\lambda} = 1$ in table 8, while for $\Lambda/m_R \geq 100$ the formula

$$\ln(\Lambda/m_R) \leq \frac{1}{\beta_1 g_R} + \frac{\beta_2}{\beta_1^2} \ln(\beta_1 g_R) - 1.9(1) \tag{4.61}$$

applies. Finally, we remark that the bound

$$m_R/v_R \leq 2.6 \quad (\text{if } \Lambda \geq 2m_R) \tag{4.62}$$

is a little lower than what we found earlier in the case $n = 1$. That the number on the r.h.s. of eq.(4.62) decreases as a function of n, is in accord with the large n result $m_R/v_R \leq O(1/\sqrt{n})$, but the amount of decrease between $n = 1$ and $n = 4$ is much smaller than what would be suggested by this formula.

We now proceed to discuss the errors in our calculations which arise from our incomplete knowledge of the Callan-Symanzik coefficients [1]. As we have pointed out at several places, the errors quoted in the tables above do not take these uncertainties into account. Because only few coefficients in the perturbative expansion of β, γ, δ and ϵ are known, a systematic error analysis is not possible, at least not with the same confidence as in the case of the

[1] We thank P. Hasenfratz for correspondence on this question

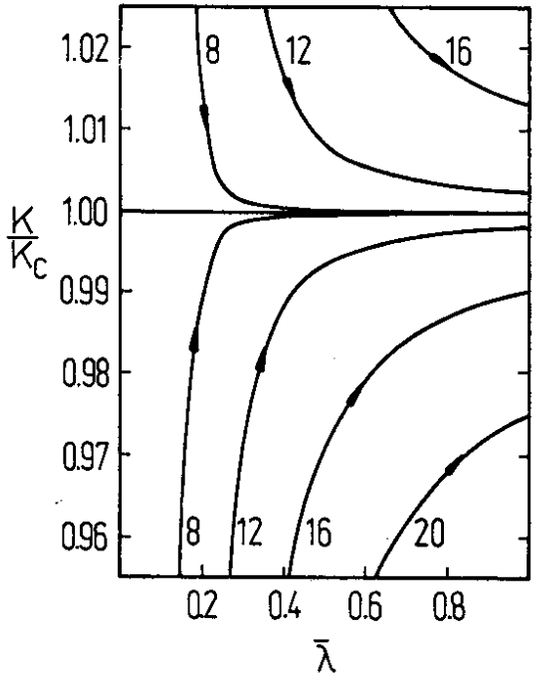

Figure 1: Quantitative drawing of renormalization group trajectories for $g_R = 8, 12, 16, 20$ and $n = 4$. The top and bottom of the diagram correspond approximately to $m_R = 0.5$ and the arrows are in the direction of decreasing m_R (i.e. increasing ultra-violet cutoff).

error estimation in the high-temperature series analysis. Still, some simple observations and tests can be made which allow one to judge the reliability of our results. For the sake of definiteness, we shall primarily discuss the case of the O(4) model and there only the possible errors implied on the evolution of the renormalized coupling g_R at $\lambda = \infty$, since this is the place where the effects are largest.

To integrate the renormalization group equation

$$m_R \frac{\partial g_R}{\partial m_R} = \beta, \tag{4.63}$$

we need to know the β-function for $0 \leq g_R \leq 20$, which, according to tables 5 and 8, is about the relevant integration range. If we neglect scaling violation terms for a moment, the perturbative expansion of the β-function may be written as

$$\beta = \beta_1 g_R^2 \left\{1 - 0.274\,(g_R/20) + c\,(g_R/20)^2 + O(g_R^3)\right\}, \qquad (4.64)$$

where $c = 0.177$ in the symmetric phase and $c = 0.079$ in the Goldstone phase. Thus, the perturbation expansion is reasonably well-behaved, in particular, the one-loop term is clearly the dominant contribution. Furthermore, as the series is apparently alternating, one may expect that the true β-function is somewhere between the 2-loop and the 3-loop curve. In the symmetric phase of the $n = 1$ model, this has actually been confirmed by a recent high precision numerical simulation [8]. Assuming the β-function indeed has this property also for $n = 4$ and in both phases, upper and lower bounds on the solution of eq.(4.63) can be derived. In this way, the total error on g_R can be estimated and one then obtains the values quoted in table 9.

Compared to the 3-loop results summarized in tables 5 and 8, the numbers in table 9 are almost the same, but the errors have increased by a factor of up to 2 in the symmetric phase and a factor between 3 and 4 in the Goldstone phase. This is also reflected in the integration constant $\ln C_1$, which we earlier estimated to be equal to 1.53(15), while one obtains 1.32(37) when the uncertainty in the β-function is included.

There are several reasons to expect that the errors quoted in table 9 are overestimated. First, it is obvious that for sufficiently small g_R, the 3-loop formula will be a better approximation to the full β-function than the 2-loop expression. Thus, if we integrate eq.(4.63) using the 3-loop formula in the range $g_R < 10$, for example, and either the 2-loop or the 3-loop formula otherwise, the errors in the Goldstone phase increase by only a factor of 2 relative to the numbers quoted in table 8, and for $\ln C_1$ one would obtain the estimate 1.42(26). The 3-loop formula actually happens to compare slightly better with the high-temperature series results than the 2-loop approximation (cf. table 6) and hence for the larger couplings too one has some reason to prefer the 3-loop formula. Furthermore, in the Goldstone phase of the $n = \infty$ model, the exact β-function (B.10) is reproduced by the 3-loop approximation within an error of at most 7% in the relevant range of couplings, while the

Table 9: Values of the renormalized coupling g_R in the symmetric phase (SP) and the Goldstone phase (GP) for $n = 4$ and $\lambda = \infty$, with errors including the uncertainties from the high-temperature expansion aswell as those arising from the perturbation expansion of the β-function.

m_R	$(g_R)_{SP}$	$(g_R)_{GP}$
0.50	26.0(6)	21(4)
0.40	22.8(8)	19(3)
0.30	20(1)	17(3)
0.20	17(1)	15(2)
0.10	13.2(9)	12(1)
0.08	12.4(8)	11(1)
0.06	11.5(7)	10(1)
0.04	10.4(6)	9.6(8)
0.02	9.0(5)	8.3(6)

2-loop curve deviates by up to 23%. Finally, the use of the 3-loop expression in the one-component model has been quite successful when the results were compared with numerical simulation data [3,7,8]. Taken together, we are thus led to believe that the true values of g_R in the O(4) model differ from the 3-loop estimates by at most twice the error quoted in tables 5 and 8. The other quantities listed in these tables are not affected significantly by the uncertainties in the Callan-Symanzik coefficients and the quoted errors should be reliable in these cases.

Recently several groups of authors have performed large scale numerical simulations of the O(4)-symmetric model in the Goldstone phase [11-18] (as far as we know, the first Monte Carlo studies of this model, addressing the question of triviality, have been made by Whitmer [9] and independently by Tsypin [10]). Although different definitions of the σ-mass and of the wave function renormalization constant Z_R have been employed, there is general agreement among the results obtained. We here choose to compare our analytic "solution" with the work of Hasenfratz et al.[15], because their definitions of v_R, Z_R and m_σ are the same as ours and the comparision is hence straightforward (see table 10). By eq.(4.44), m_σ is equal to m_R

Table 10: Comparision between numerical simulation data from ref.[15] (first line for given λ and κ) and our analytic results (second line).

λ	κ	m_R	g_R	Z_R
0.05	0.1505	0.42(1)	6.8(4)	-
0.05	0.15059(9)	0.42	6.9(2)	3.296(2)
1.00	0.2520	0.50(1)	15.8(4)	-
1.00	0.2525(4)	0.50	15(1)	1.947(6)
∞	0.3100	0.43(1)	20(1)	1.55(2)
∞	0.3109(5)	0.43	18(2)	1.568(9)
∞	0.3075	0.33(1)	19(1)	1.56(2)
∞	0.3083(3)	0.33	16(2)	1.578(9)

to a very good approximation at all points considered so that we have set $m_R = m_\sigma$ throughout. The selection of the data has been such that only masses $m_R \leq 0.5$ were considered and for given λ and κ we only quote the result obtained on the largest lattice so that we hope finite size effects are small (in all cases, the lattice size is at least 5 times as large as the Compton wave length of the σ-particle). For $\lambda = 0.05$ and $\lambda = 1.00$, the wave function renormalization constant Z_R was not measured but it was assumed in ref.[15] to be equal to $1/2\kappa$ (which is an excellent approximation according to the analytic solution). At every point, the values of λ and m_R are taken as input to the analytic calculation which then predicts κ, g_R and Z_R. For the Callan-Symanzik coefficients we have used the 3-loop expressions and doubled the errors on g_R to account for the uncertainty in the β-function as discussed above.

As shown by table 10, the agreement between the Monte Carlo data and our analytic results is rather good, especially at the lower values of λ. At $\lambda = \infty$, our "prediction" for the coupling g_R seems to be systematically lower than the Monte Carlo result, but the effect is barely significant and one should also keep in mind that the numerical determination of a resonance

mass is far from trivial because the energy eigenvalue in finite volume which corresponds to the resonance has a complicated lattice size dependence (see refs.[20,21] for more details). In any case, the matching of the two methods of calculation is remarkable and little doubt remains that any one of them is basically correct. Thus, a rather detailed solution of the four-component model has been achieved in this way and, recalling the earlier results on the $n = 1$ and the $n = \infty$ case, one may safely expect that the behaviour of the model for general n is qualitatively similar.

4.7 Example of Finite Cutoff Effects in Physical Amplitudes

Although we do not expect the lattice to provide a realistic ultra-violet cutoff in any theory of real elementary particles, it is nevertheless interesting to know at which energies the presence of this cutoff would have a sizeable influence on the scattering processes of the Goldstone bosons. If one wants to compare different regularization schemes (in particular the associated triviality bounds on the renormalized coupling as in refs.[16-18]) the cutoff masses should be matched in such a way that the cutoff effects in the theories considered are about the same in a range of energy close to the cutoff. Of course, this specification is not a very precise one, but as we shall see below, cutoff effects tend to be small up to a certain energy and then rise dramatically, i.e. this rapid onset allows one to define a "phenomenological" cutoff scale up to a factor of 2 or so.

We first consider elastic scattering processes of Goldstone bosons at energies well above the σ-resonance. At tree-level of perturbation theory and in the limit of vanishing pion mass (i.e. for $h = 0$), the scattering amplitude in the centre-of-mass system is given by [1]

$$T(\mathbf{p}'a', \mathbf{q}'b' \mid \mathbf{p}\,a, \mathbf{q}\,b) =$$
$$Z(\mathbf{p})Z(\mathbf{p}')\left\{\delta_{ab}\delta_{a'b'}A(\hat{s}) + \delta_{aa'}\delta_{bb'}A(\hat{t}) + \delta_{ab'}\delta_{ba'}A(\hat{u})\right\}. \qquad (4.65)$$

The notation here is as follows. The in-going particles have momenta $\mathbf{p}$ and $\mathbf{q} = -\mathbf{p}$, and their $O(n-1)$ labels are a and b. Primed momenta and symmetry labels refer to the out-going state. To leading order in g_R, the energy $\omega(\mathbf{p}) \geq 0$ of a single Goldstone boson with momentum $\mathbf{p}$ is determined

[1] For a discussion of particle scattering in lattice field theories see sect.2 of ref.[21].

by

$$\cosh\omega(\mathbf{p}) = 1 + \sum_{k=1}^{3}(1 - \cos p_k), \tag{4.66}$$

and energy conservation thus requires $\omega(\mathbf{p}) = \omega(\mathbf{p}')$. On the lattice the on-shell wave function renormalization constant $Z(\mathbf{p})$ is momentum dependent. Explicitly, we have

$$Z(\mathbf{p}) = \omega(\mathbf{p})/\sinh\omega(\mathbf{p}) + O(g_R). \tag{4.67}$$

Finally, the amplitude A in eq.(4.65) is given by

$$A(z) = \frac{1}{3} g_R \frac{m^2}{m_R^2} \frac{z}{m^2 - z}, \tag{4.68}$$

where

$$m^2 = 2(\cosh m_R - 1), \tag{4.69}$$

and the lattice Mandelstam variables $\hat{s}$, $\hat{t}$ and $\hat{u}$ are defined through

$$\hat{s} = 2\{\cosh 2\omega(\mathbf{p}) - 1\}, \tag{4.70}$$

$$\hat{t} = -2\sum_{k=1}^{3}\{1 - \cos(p'_k - p_k)\}, \tag{4.71}$$

$$\hat{u} = -2\sum_{k=1}^{3}\{1 - \cos(p'_k + p_k)\}. \tag{4.72}$$

For the differential cross-section for Goldstone boson scattering we now obtain

$$\frac{d\sigma}{d\Omega} = \frac{\mathbf{p}'^2}{16\pi^2}\left\{(2\sinh W/2)^4\,|\omega'(\mathbf{p})\omega'(\mathbf{p}')|\right\}^{-1} \times\left\{(n-2)A(\hat{s})^2 + (A(\hat{s}) + A(\hat{t}) + A(\hat{u}))^2\right\}, \tag{4.73}$$

where W is the total energy,

$$W = 2\omega(\mathbf{p}), \tag{4.74}$$

and ω' is given by

$$\omega'(\mathbf{p}) = \frac{1}{|\mathbf{p}|}\,\mathbf{p}\cdot\nabla\omega(\mathbf{p}). \tag{4.75}$$

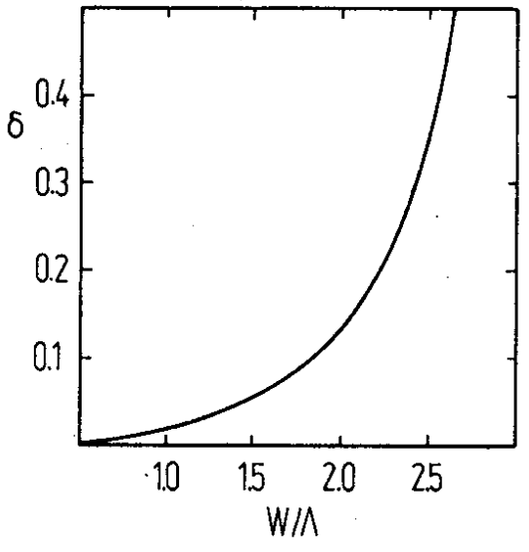

Figure 2: Deviaton $\delta = (\frac{d\sigma}{d\Omega})_{\rm latt}/(\frac{d\sigma}{d\Omega})_{\rm cont} - 1$ between the lattice and continuum differential cross-sections for Goldstone boson scattering at 90° versus the total centre-of-mass energy W.

The comparision of eq.(4.73) with the corresponding continuum expression for the differential cross-section reveals that the biggest cutoff effects apparently occur for a scattering angle $\theta = 90°$. This is illustrated in fig.2 for $n = 4$ and $m_R = 0.5$ (the coupling g_R drops out in the ratio of cross-sections plotted and it is therefore not necessary to specify its value). It can be shown that the deviation is not very sensitively dependent on m_R. In fact, it mainly stems from the kinematic pre-factor in eq.(4.73), which in turn reflects the order of magnitude of the cutoff effects in the energy-momentum relation (4.66).

At energies around and below the σ-resonance, the Goldstone scattering amplitude is mainly determined by the resonance mass m_σ and width Γ_σ. As our second example of cutoff effects, we thus consider the σ-width defined by

eq.(4.43). To lowest order of perturbation theory, it is given by

$$\Gamma_\sigma = \frac{1}{6}(n-1)g_R \frac{m^4}{m_R^2 \sinh m_R} \mathrm{Im\,I}, \tag{4.76}$$

where I denotes the lattice one-loop integral

$$\mathrm{I} = \int_{-\pi}^{\pi} \frac{d^4q}{(2\pi)^4} \left\{ ((q+\widehat{p}/2)^2 + m^2)((q-\widehat{p}/2)^2 + m^2) \right\}^{-1} \Big|_{p=(im_R-\varepsilon,0,0,0)} \tag{4.77}$$

(recall that $m_\sigma = m_R$ to the order considered). Performing the q_0 integration, we have

$$\mathrm{Im\,I} = \frac{\pi}{m^2} \int_{-\pi}^{\pi} \frac{d^3q}{(2\pi)^3}\, \delta(2\omega(\mathbf{q}) - m_R). \tag{4.78}$$

Numerical integration now shows that the cutoff effects in this lowest order formula for Γ_σ are rather small ($< 1\%$) for $m_R \leq 0.5$; they reach around 10% at $m_R = 2$ and from thereon grow dramatically.

Summarizing, we find that for $m_R/\Lambda \leq 0.5$ and centre-of-mass energies $W \leq \Lambda$, the cutoff effects in the elastic scattering cross section are at the few percent level at most. In the region $\Lambda < W \leq 2\Lambda$, however, there is a rapid growth and for $W > 2\Lambda$ the effects are large.

Appendix A

Perturbation Expansion of the Callan-Symanzik Coefficients β, γ and δ in the Symmetric Phase

The method of calculation is exactly the same as in the one-component model (appendix A of (I)) so that here we merely quote the results. The universal coefficients β_ν, γ_ν and δ_ν, as defined through eqs.(I.A.1)-(I.A.3), are given up to three loops by

$$\beta_1 = \frac{1}{3}(n+8)(16\pi^2)^{-1}, \tag{A.1}$$

$$\beta_2 = -\frac{1}{3}(3n+14)(16\pi^2)^{-2}, \tag{A.2}$$

$$\beta_3 = \frac{1}{432}\{61n^2 + 1782n + 5744 + 192\zeta(3)(5n+22) - 2k(n+8)(13n+62)\}(16\pi^2)^{-3}, \tag{A.3}$$

$$\gamma_1 = 0, \tag{A.4}$$

$$\gamma_2 = \frac{1}{36}(n+2)(16\pi^2)^{-2}, \tag{A.5}$$

$$\gamma_3 = -\frac{1}{432}(n+2)(n+8)(1-2k)(16\pi^2)^{-3}, \tag{A.6}$$

$$\delta_1 = -\frac{1}{3}(n+2)(16\pi^2)^{-1}, \tag{A.7}$$

$$\delta_2 = \frac{5}{18}(n+2)(16\pi^2)^{-2}, \tag{A.8}$$

$$\delta_3 = -\frac{1}{216}(n+2)\{31n + 221 + 6k(n+1)\}(16\pi^2)^{-3}. \tag{A.9}$$

The Riemann zeta function $\zeta(3)$ and the constant k appearing above are given numerically by

$$\zeta(3) = 1.20205690, \tag{A.10}$$

$$k = 1.62520965. \tag{A.11}$$

Concerning the full m_R-dependent coefficients u_ν, v_ν and w_ν, defined through eqs.(I.A.4)-(I.A.6), we first note that the tree-level coefficients are independent of n. Thus, eqs.(I.A.7), (I.A.9) and (I.A.11) remain valid for all n. For the one-loop coefficients we have

$$u_1 = \frac{1}{6}u_0\Big\{(n+8)(8+m_R^2)J_3(m_R) - 6J_2(m_R) - (n+2)\frac{J_1(m_R)}{8+m_R^2}\Big\}, \tag{A.12}$$

$$v_1 = \frac{1}{24}(n+2)u_0\Big\{J_2(m_R) - \frac{J_1(m_R)}{8+m_R^2}\Big\}, \tag{A.13}$$

$$w_1 = -2v_1 - \frac{1}{12}(n+2)m_R^2\Big\{(8+m_R^2)J_3(m_R) - 2J_2(m_R) + \frac{J_1(m_R)}{8+m_R^2}\Big\}, \tag{A.14}$$

where the integrals $J_p(\mu)$ appearing in these equations are the same as in (I) (cf. eq.(I.A.13) and appendix B of (I)).

Appendix B

PERTURBATION EXPANSION OF THE CALLAN-SYMANZIK COEFFICIENTS β, γ, δ AND ϵ IN THE BROKEN SYMMETRY PHASE

In this appendix we specify the renormalization group functions appropriate to our renormalization scheme in the broken symmetry phase to 3-loop order for $h = 0$ and all $n \geq 2$. The coefficients $\beta_1, \beta_2, \gamma_1$ and δ_1 are the same as in the symmetric phase (eqs.(A.1),(A.2),(A.4) and (A.7)), while the remaining universal coefficients are

$$\begin{aligned} \beta_3 &= \{-\frac{\pi^2}{108}n^3 - 0.6038002\,n^2 \\ &\quad + 6.006124\,n + 11.10641\}(16\pi^2)^{-3}, \end{aligned} \tag{B.1}$$

$$\gamma_2 = -\frac{1}{6}(16\pi^2)^{-2}, \tag{B.2}$$

$$\gamma_3 = \{-0.0452317896\,n + 0.211712032\}(16\pi^2)^{-3}, \tag{B.3}$$

$$\delta_2 = \frac{1}{18}\{(5 + 2\sqrt{3}\pi)\,n16 - 2\sqrt{3}\pi\}(16\pi^2)^{-2}, \tag{B.4}$$

$$\begin{aligned} \delta_3 &= \{\frac{\pi^2}{108}\,n^3 + 1.2932334\,n^2 \\ &\quad - 4.320590\,n + 1.620019\}(16\pi^2)^{-3}. \end{aligned} \tag{B.5}$$

For the coefficient ϵ, we have

$$\epsilon(0, g_R) = \sum_{\nu=0}^{\infty} \epsilon_\nu g_R^\nu, \tag{B.6}$$

$$\epsilon_0 = 1, \tag{B.7}$$

$$\epsilon_1 = \frac{1}{6}\{-n + 3 - 2\sqrt{3}\pi)\}(16\pi^2)^{-1}, \tag{B.8}$$

$$\epsilon_2 = \{0.503662\,n + 2.487506\}(16\pi^2)^{-2}. \tag{B.9}$$

Note that contrary to what happens in the symmetric phase, the 3-loop coefficient of the β-function here does not vanish in the $n \to \infty$ limit with

$\hat{g}_R \equiv n g_R$ fixed. Indeed, the β-function can be computed exactly in this limit and its universal part is given by

$$n\beta(0, g_R) = \frac{\hat{g}_R^2}{24\pi^2}\left\{1 + (1 - z^2)^{-1/2}\right\}^{-1}, \tag{B.10}$$

where $z = \hat{g}_R/48\pi$. This beta function has a zero at $\hat{g}_R = 48\pi$ which coincides with the value of the tree-level unitarity bound (4.42). Since $\hat{g}_R$ is always smaller than 35π in the scaling region, this zero has, however, no particular significance regarding the triviality of the $n = \infty$ theory.

For the full m_R-dependent coefficients u_ν, v_ν, w_ν defined in eqs.(I.A.4)-(I.A.6) and x_ν defined similarly through

$$\epsilon(m_R, g_R) = \sum_{\nu=0}^{\infty} x_\nu(m_R) g_R^\nu, \tag{B.11}$$

we have up to one-loop order

$$u_0 = 2 - m_R\sqrt{1 + s^{-2}} - m_R\frac{\sinh m_R}{4 - s^2}, \tag{B.12}$$

$$\begin{aligned} u_1 &= \beta_1 + m_R^2\Big\{-\ln m_R^2 + 3.780265 \\ &\quad + 0.214721\,n\Big\}(16\pi^2)^{-1} + O(m_R^4 \ln m_R^2), \end{aligned} \tag{B.13}$$

$$v_0 = -\frac{1}{4}m_R\frac{\sinh m_R}{4 - s^2}, \tag{B.14}$$

$$\begin{aligned} v_1 &= m_R^2\Big\{\frac{1}{96}(n + 2)\ln m_R^2 + 0.110107 \\ &\quad - 0.018060\,n\Big\}(16\pi^2)^{-1} + O(m_R^4 \ln m_R^2), \end{aligned} \tag{B.15}$$

$$w_0 = m_R \sinh m_R \frac{s^2}{16 - s^4}, \tag{B.16}$$

$$\begin{aligned} w_1 &= \delta_1 + m_R^2\Big\{\frac{1}{24}(n + 2)\ln m_R^2 - 0.025718 \\ &\quad - 0.159533\,n\Big\}(16\pi^2)^{-1} + O(m_R^4 \ln m_R^2), \end{aligned} \tag{B.17}$$

$$x_0 = \frac{\sinh m_R}{m_R}\frac{4 + s^2}{4 - s^2}, \tag{B.18}$$

$$x_1 = \epsilon_1 + m_R^2\Big\{\frac{1}{2}\ln m_R^2 - 2.029726 - 0.121250\,n\Big\}(16\pi^2)^{-1} + O(m_R^4 \ln m_R^2), \qquad \text{(B.19)}$$

where the abbreviation $s = \sinh(m_R/2)$ has been used. For the one-loop expressions we have above only specified the leading cutoff dependences; these are in some cases rather substantial, but we have verified that they approximate the full cutoff effects rather well in the range $m_R \leq 0.5$.

Appendix C

Continuum Limit of Lattice One-Loop Integrals

At several places in this work, it was necessary to perform explicit perturbative calculations on the lattice to one-loop order. In the symmetric phase, the Feynman diagrams encountered in these calculations have always vanishing external momenta and they can thus be reduced to a combination of the integrals $J_p(\mu)$, which we have introduced and analyzed in (I). Because the renormalization conditions in the Goldstone phase involve the external momentum

$$p = (i\,m_R - \epsilon, 0, 0, 0) \qquad \text{(C.1)}$$

($\epsilon > 0$, infinitesimal), three new integrals occur whose continuum limit and leading lattice corrections must be worked out.

If we define a parameter $m > 0$ through

$$m^2 = 2(\cosh m_R - 1), \qquad \text{(C.2)}$$

the new integrals can be written as

$$K_1(m) = \int_{-\pi}^{\pi} \frac{d^4q}{(2\pi)^4} \Big\{(\hat{q}_+^2 + m^2)(\hat{q}_-^2 + m^2)\Big\}^{-1}, \qquad \text{(C.3)}$$

$$K_2(m) = \mathrm{Re} \int_{-\pi}^{\pi} \frac{d^4q}{(2\pi)^4} (\hat{q}_+^2 \hat{q}_-^2)^{-1}, \qquad \text{(C.4)}$$

$$K_3(m) = \int_{-\pi}^{\pi} \frac{d^4q}{(2\pi)^4}\, m^2 \sum_{\mu=0}^{3} (\sin q_\mu)^2 \Big\{\hat{q}^2(\hat{q}^2 + m^2)\Big\}^{-2}. \qquad \text{(C.5)}$$

In these equations, we have used the abbreviation

$$q_\pm = q \pm p/2, \qquad \text{(C.6)}$$

and m_R is considered a function of m via eq.(C.2).

For $m \to 0$, i.e. in the continuum limit, the integrals K_i can be expanded in an asymptotic series of m^{2k} and $m^{2k}\ln m^2$ ($k = 0, 1, 2, \ldots$). The first few terms in these expansions are

$$K_1(m) = \frac{1}{16\pi^2}\Big\{-\ln m^2 + a_1 + \frac{1}{4}m^2 \ln m^2 + b_1 m^2 + O(m^4 \ln m^2)\Big\}, \qquad \text{(C.7)}$$

$$K_2(m) = \frac{1}{16\pi^2}\Big\{-\ln m^2 + a_2 + b_2 m^2 + O(m^4 \ln m^2)\Big\}, \qquad \text{(C.8)}$$

$$K_3(m) = \frac{1}{16\pi^2}\Big\{a_3 + b_3 m^2 + O(m^4 \ln m^2)\Big\}. \qquad \text{(C.9)}$$

In these equations, the coefficients a_i and b_i can be expressed in terms of three other numbers c_1, c_2 and c_3 through

$$a_1 = c_1 + 2 - \frac{\pi}{\sqrt{3}}, \qquad \text{(C.10)}$$

$$b_1 = c_2 - c_3 - \frac{1}{6} + \frac{\pi}{12\sqrt{3}}, \qquad \text{(C.11)}$$

$$a_2 = c_1 + 2, \qquad \text{(C.12)}$$

$$b_2 = -c_3 + \frac{1}{12}, \qquad \text{(C.13)}$$

$$a_3 = 1, \qquad \text{(C.14)}$$

$$b_3 = -2c_3, \qquad \text{(C.15)}$$

and, finally, the numbers c_i are given by

$$c_1 = 3.79200957, \qquad \text{(C.16)}$$

$$c_2 = -0.75171379, \qquad \text{(C.17)}$$

$$c_3 = \frac{1}{48}(2c_1 + 8c_2 + 1). \qquad \text{(C.18)}$$

c_1 and c_2 are related to the coefficients r_1 and r_2 which appear in the expansion (I.B.1),(I.B.2) of the integrals $J_p(\mu)$ through

$$c_1 = -16\pi^2 r_1 - 1, \qquad \text{(C.19)}$$

$$c_2 \;=\; -32\pi^2 r_2 + \frac{1}{8}. \qquad \text{(C.20)}$$

To prove eq.(C.7), we have first considered the integral K_1 for an arbitrary momentum p of order m. It is then possible to show that the subtracted integral

$$K_1'(m,p) = [1 - T_2(p)]K_1(m,p), \qquad \text{(C.21)}$$

where $T_2(p)$ denotes the Taylor operator of order 2, converges in the continuum limit with a rate of convergence proportional to $m^4 \ln m^2$. Since the subtractions $T_2(p)K_1(m,p)$ are at zero momentum, they can be reduced to a combination of the integrals $J_k(m)$ which we already know how to expand for $m \to 0$. In this way, one obtains for the unsubtracted integral

$$\begin{aligned} K_1(m,p) \;&=\; \frac{1}{16\pi^2}\Big\{c_1 + X_1(m,p) + \frac{1}{4}m^2 \ln m^2 \\ &\quad + m^2 c_2 + p^2 c_3 + X_2(m,p) + O(m^4 \ln m^2)\Big\}, \end{aligned} \qquad \text{(C.22)}$$

where the continuum integrals X_1 and X_2 are defined through

$$X_1 \;=\; -\int_0^1 ds\, \ln[m^2 + s(1-s)p^2], \qquad \text{(C.23)}$$

$$\begin{aligned} X_2 \;&=\; -\frac{1}{24}\int_0^1 ds\, s(1-s)[m^2 + s(1-s)p^2]^{-1} \\ &\quad \times\Big\{3(1-2s)^2(p^2)^2 - 4s^3 \sum_{\mu=0}^{3} p_\mu^4\Big\}. \end{aligned} \qquad \text{(C.24)}$$

By setting p to the desired value (C.1), eq.(C.7) now follows trivially.

The proof of the other expansions (C.8) and (C.9) proceeds similarly, in fact both cases can be algebraically reduced to the integrals already considered.

References

1. M. Lüscher and P. Weisz, Nucl. Phys. B290 [FS20] (1987) 25
2. M. Lüscher and P. Weisz, Nucl. Phys. B295 [FS21] (1988) 65
3. M. Lüscher, "Solution of the lattice ϕ^4 theory in 4 dimensions", DESY 87-159, lectures at the Cargèse Summer School 1987, to be published in the proceedings
4. M. Lüscher and P. Weisz, Nucl. Phys. B300 [FS22] (1988) 325
5. M. Lüscher and P. Weisz, "Is there a strong interaction sector in the standard lattice Higgs model?", DESY 88-083, to appear in Phys. Lett. B
6. E. Brézin, J. C. Le Guillou and J. Zinn-Justin, "Field theoretical approach to critical phenomena", *in* Phase transitions and critical phenomena, vol. 6, eds. C. Domb, M. S. Green (Academic Press, London, 1976)
7. I. Montvay and P. Weisz, Nucl. Phys. B290 [FS20] (1987) 327
8. I. Montvay, G. Münster and U. Wolff, "Percolation cluster algorithm and scaling behaviour in the 4-dimensional Ising model", DESY 88-049, to be published in Nucl. Phys. B
9. C. Whitmer, Princeton University Ph. D. Dissertation (1983)
10. M. M. Tsypin, "The effective potential of the lattice ϕ^4 theory and the upper bound on the Higgs mass", Lebedev Physical Institute preprint 280, 1985
11. J. Kuti and Y. Shen, Phys. Rev. Lett. 60 (1988) 85,
12. J. Kuti, L. Lin and Y. Shen, Phys. Rev. Lett. 61 (1988) 678,
13. J. Kuti, L. Lin and Y. Shen, "Non-perturbative study of the Higgs sector in the Standard Model", San Diego Preprint, UCSD/PTH-88-05
14. A. Hasenfratz, K. Jansen, C. B. Lang, T.Neuhaus and H. Yoneyama, Phys. Lett. 199B (1987) 531

15. A. Hasenfratz, K. Jansen, J. Jersák, C. B. Lang, T.Neuhaus and H. Yoneyama, "Study of the 4-component Φ^4 model", Jülich preprint, HLRZ-88-02

16. G. Bhanot and K. Bitar, Phys. Rev. Lett. 61 (1988) 798

17. G. Bhanot and K. Bitar, " Lattice Higgs mass bounds and different cutoff schemes", Florida preprint, FSU-SCRI-88-C-52

18. G. Bhanot, "How reliable are the lattice Higgs mass bounds?", Talk given at Symposium on Lattice field theory 1988, Fermilab, Batavia, to be published

19. W. Bernreuther, M. Göckeler and M. Kremer, Nucl. Phys. B295 [FS21] (1988) 211

20. U. Wiese, Talk given at Symposium on Lattice field theory 1988, Fermilab, Batavia, to be published

21. M. Lüscher, "Selected topics in lattice quantum field theory", Les Houches lectures, July 1988, to be published

22. G. A. Baker and J. M. Kincaid, J. Stat. Phys. 24 (1981) 469

23. B. W. Lee, C. Quigg and H. B. Thacker, Phys. Rev. D16 (1977) 1519

24. W. J. Marciano and S. S. D. Willenbrock, "Radiative corrections to heavy Higgs production and decays", Brookhaven preprint, BNL-40513 (1987)

25. K. Symanzik, Comm. Math. Phys. 16 (1970) 48